SUPPORTING INFORMATION

Multi-Stimuli Responsive Block Copolymers as Smart Release Platform for a Polypyridyl Ruthenium Complex

Michael Appold[a], Cristina Mari[b], Christina Lederle[c], Johannes Elbert[a,†], Claudia Schmidt[d], Ingo Ott[d], Bernd Stühn[c], Gilles Gasser[e,*], and Markus Gallei[a,*]

Corresponding authors: m.gallei@mc.tu-darmstadt.de; gilles.gasser@chimie-paristech.fr

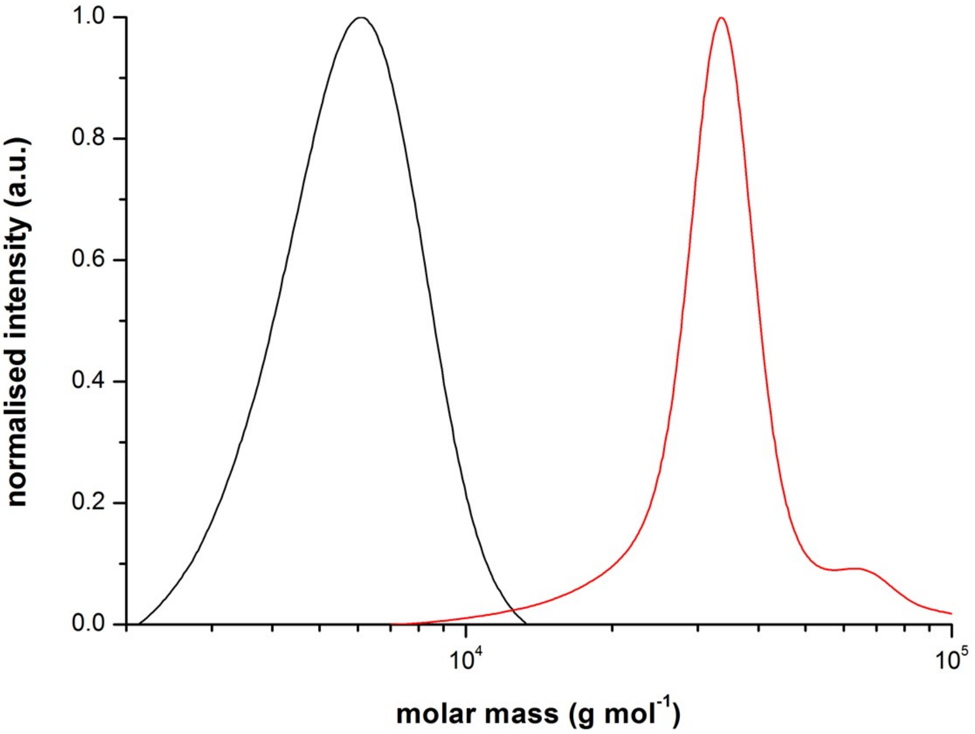

Figure S1. Molar mass distributions obtained by SEC measurements vs. PMMA standards in DMF obtained for the $PMMA_{13}$-*co*-$PDMAEMA_{22}$ precursor (black line) and the corresponding ($PMMA_{13}$-*co*-$PDMAEMA_{22}$)-*b*-$PDMAEMA_{132}$ BCP (red).

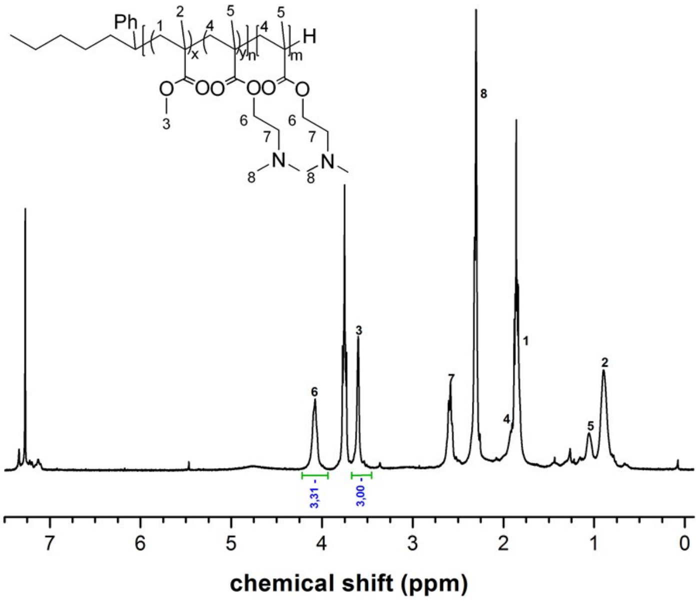

Figure S2. ^{1}H NMR spectrum of (PMMA$_{13}$-*co*-PDMAEMA$_{22}$)-*b*-PDMAEMA$_{132}$ in CDCl$_3$.

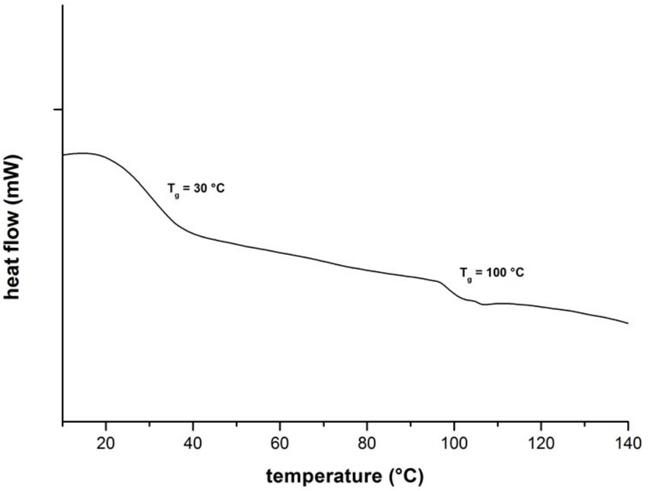

Figure S3. DSC thermogram of (PMMA$_{13}$-*co*-PDMAEMA$_{22}$)-*b*-PDMAEMA$_{132}$. The applied heat rate for the DSC run was 10 K min^{-1}.

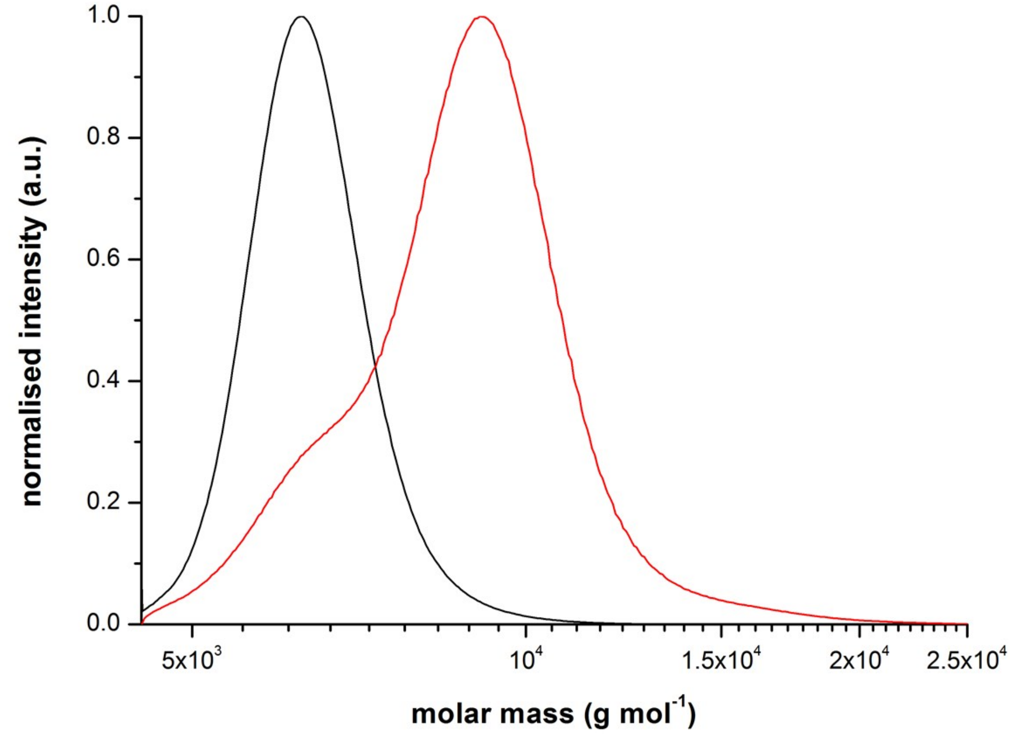

Figure S4. Molar mass distributions obtained by SEC measurements vs. PMMA standards in DMF obtained for the $PMMA_{63}$ precursor (black line) and the corresponding $PMMA_{63}$-*b*-$PDMAEMA_{25}$ BCP (red).

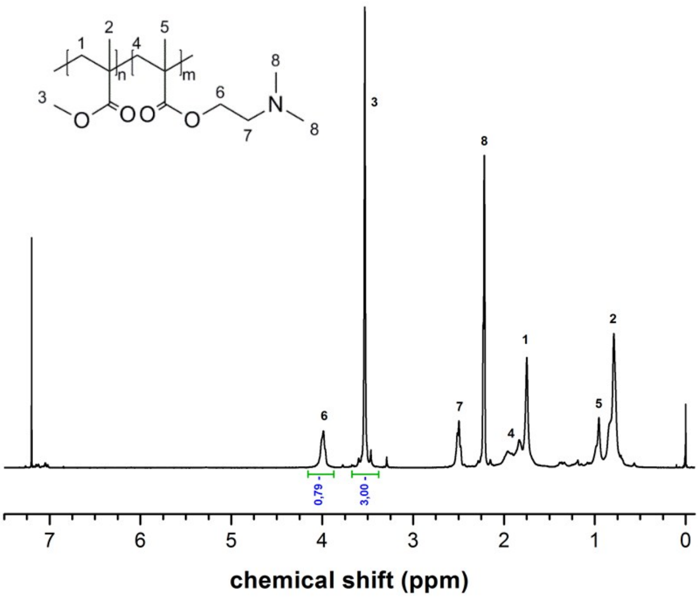

Figure S5. ^1H NMR spectrum of $PMMA_{63}$-*b*-$PDMAEMA_{25}$ in $CDCl_3$.

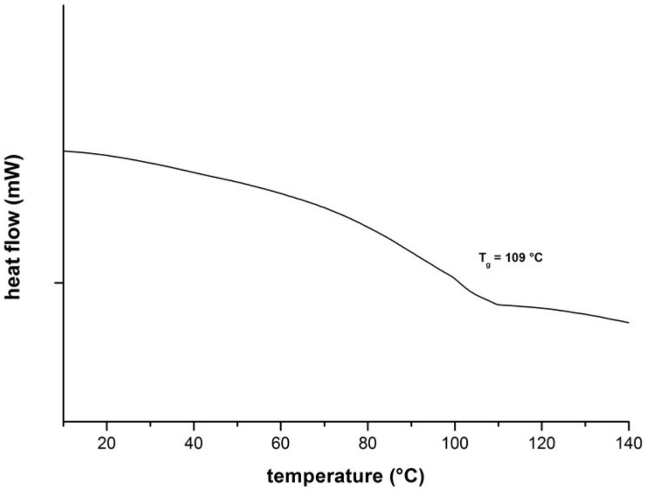

Figure S6. DSC thermogram of PMMA$_{63}$-*b*-PDMAEMA$_{25}$. The applied heat rate for the DSC run was 10 K min^{-1}.

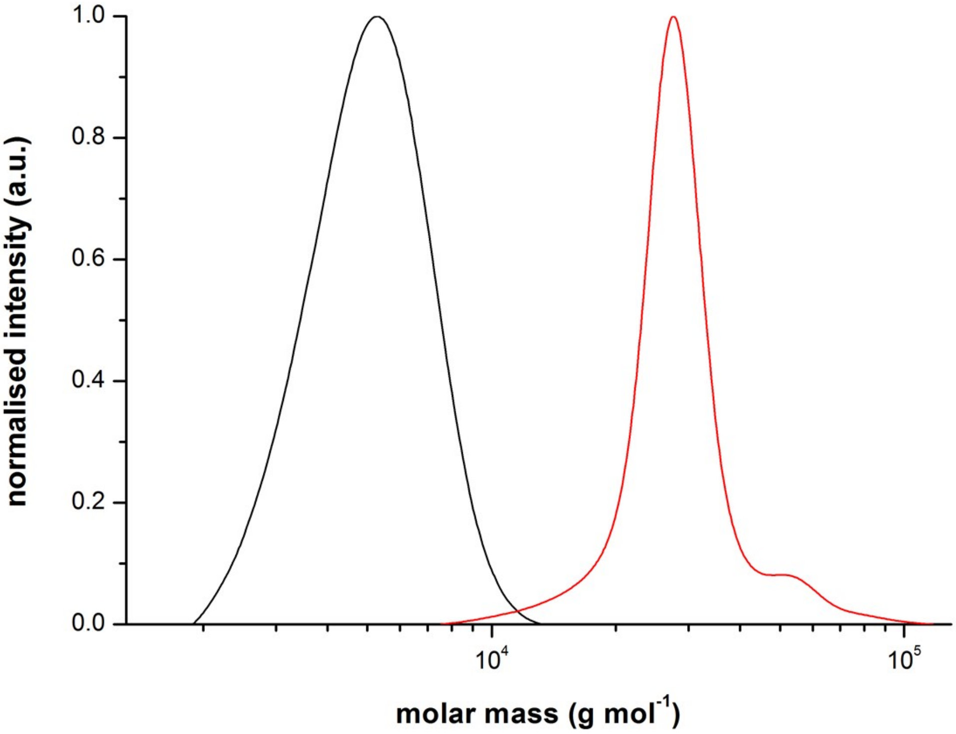

Figure S7. Molar mass distributions obtained by SEC measurements vs. PMMA standards in DMF obtained for the PMMA$_{19}$-*co*-PDMAEMA$_{22}$ precursor (black line) and the corresponding (PMMA$_{19}$-*co*-PDMAEMA$_{22}$)-*b*-PDMAEMA$_{191}$ BCP (red).

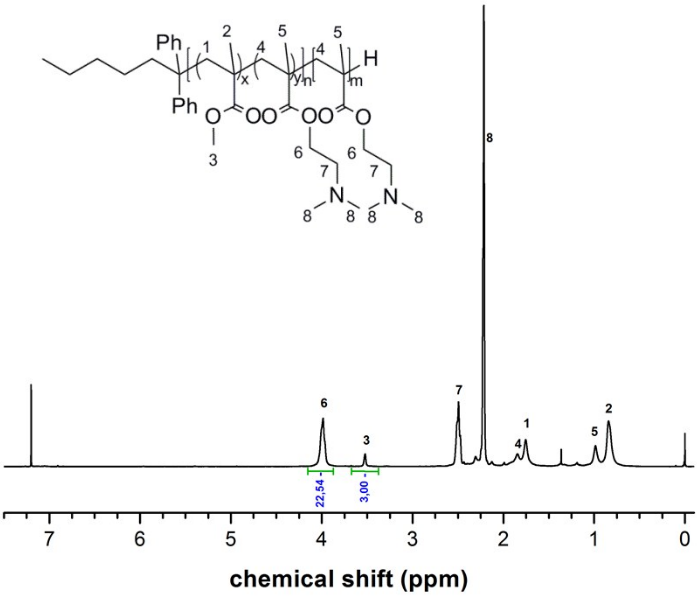

Figure S8. ^{1}H NMR spectrum of (PMMA$_{19}$-*co*-PDMAEMA$_{22}$)-*b*-PDMAEMA$_{191}$ in CDCl$_3$.

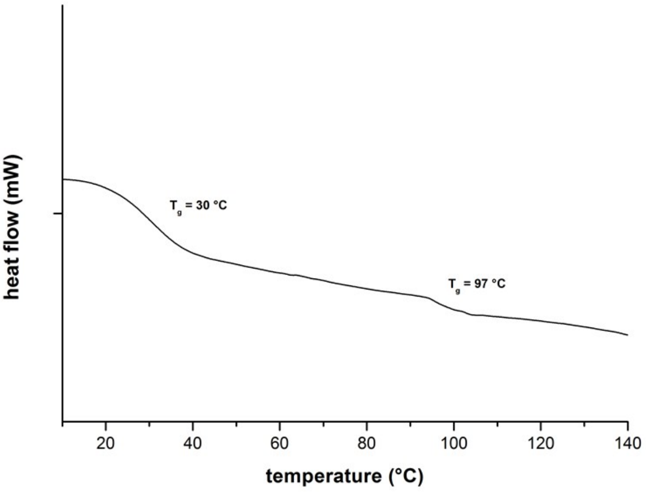

Figure S9. DSC thermogram of (PMMA$_{19}$-*co*-PDMAEMA$_{22}$)-*b*-PDMAEMA$_{191}$. The applied heat rate for the DSC run was 10 K min^{-1}.

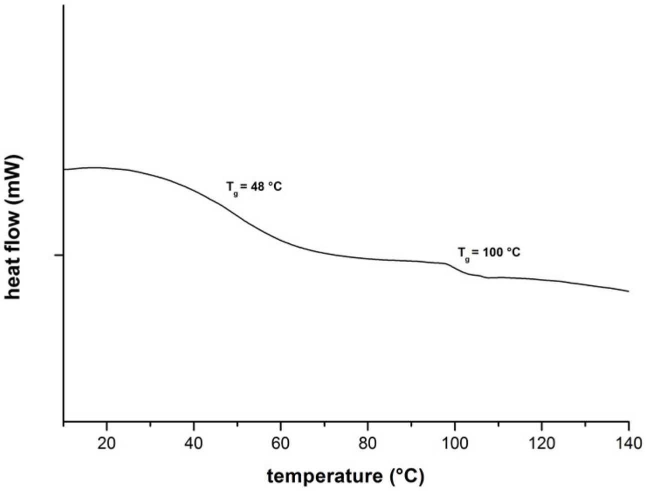

Figure S10. DSC thermogram of PMMA$_{54}$-*b*-PDMAEMA$_{95}$. The applied heat rate for the DSC run was 10 K min^{-1}.

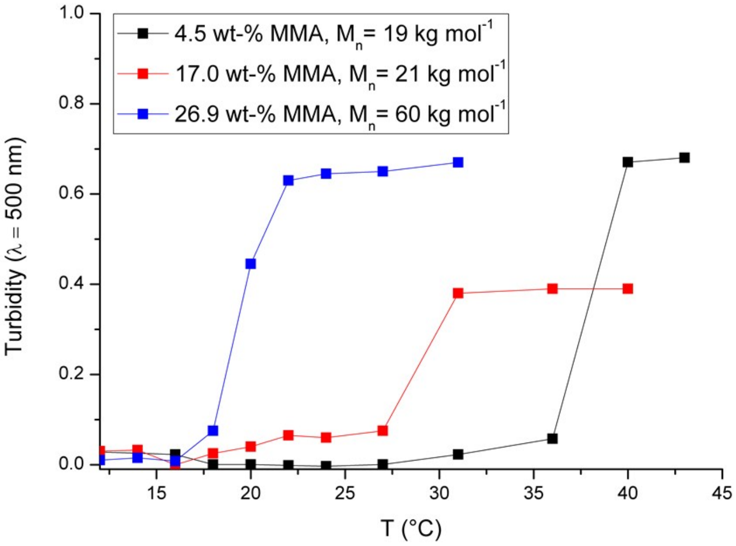

Figure S11. Results on turbidity measurements for statistical PDMAEMA-*co*-PMMA copolymers featuring different amounts of MMA.

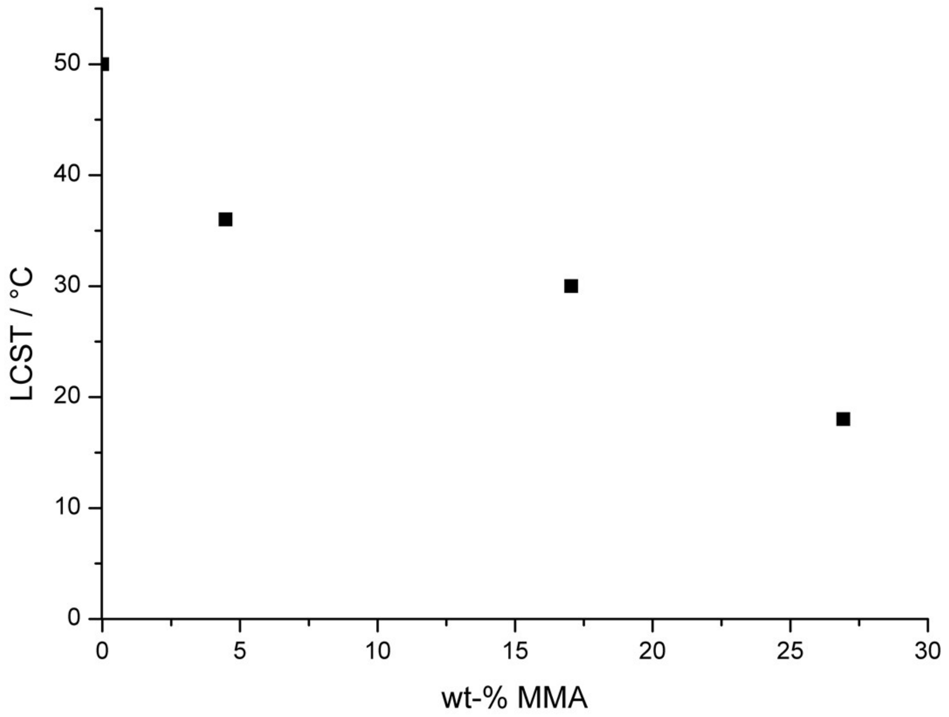

Figure S12. Correlation of MMA content as part of the statistical PDMAEMA-*co*-PMMA copolymers featuring different amounts of MMA with the LCST (see also Figure S11).

Table S1. Characterization of BCPs used in this study with respect to glass transition (T_g) temperature and lower critical solution temperature (LCST).

polymer	T_{g1} (°C)[a]	T_{g2} (°C)[a]	$LCST_1$ (°C)	$LCST_2$ (°C)
$PMMA_{63}$-*b*-$PDMAEMA_{25}$	109	-	-	55
$PMMA_{54}$-*b*-$PDMAEMA_{95}$	100	48	-	55
($PMMA_{19}$-*co*-$PDMAEMA_{22}$)-*b*-$PDMAEMA_{191}$	97	30	7	55
($PMMA_{13}$-*co*-$PDMAEMA_{22}$)-*b*-$PDMAEMA_{132}$	100	30	22	55

[a] T_g determined by DSC measurements in °C.

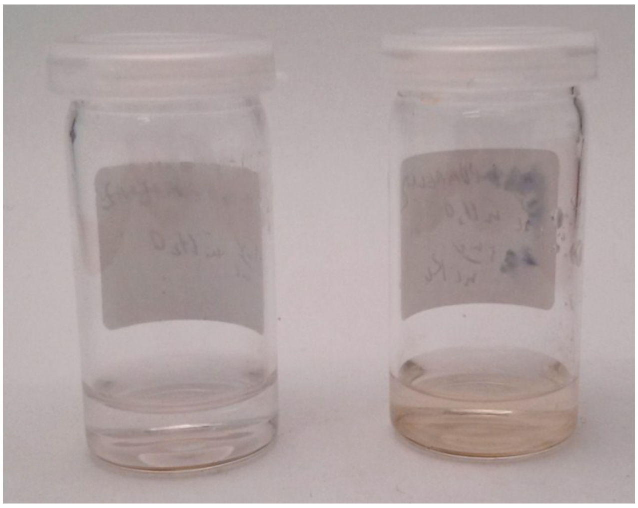

Figure S13. Photograph of PDMAEMA-containing BCP micelles after dialysis in water. In the case micelles loaded with [Ru(bipy)$_2$-dppz-7-hydroxymethyl][PF$_6$]$_2$ complex **7**, the solution featured a slightly yellow to orange colour (right).

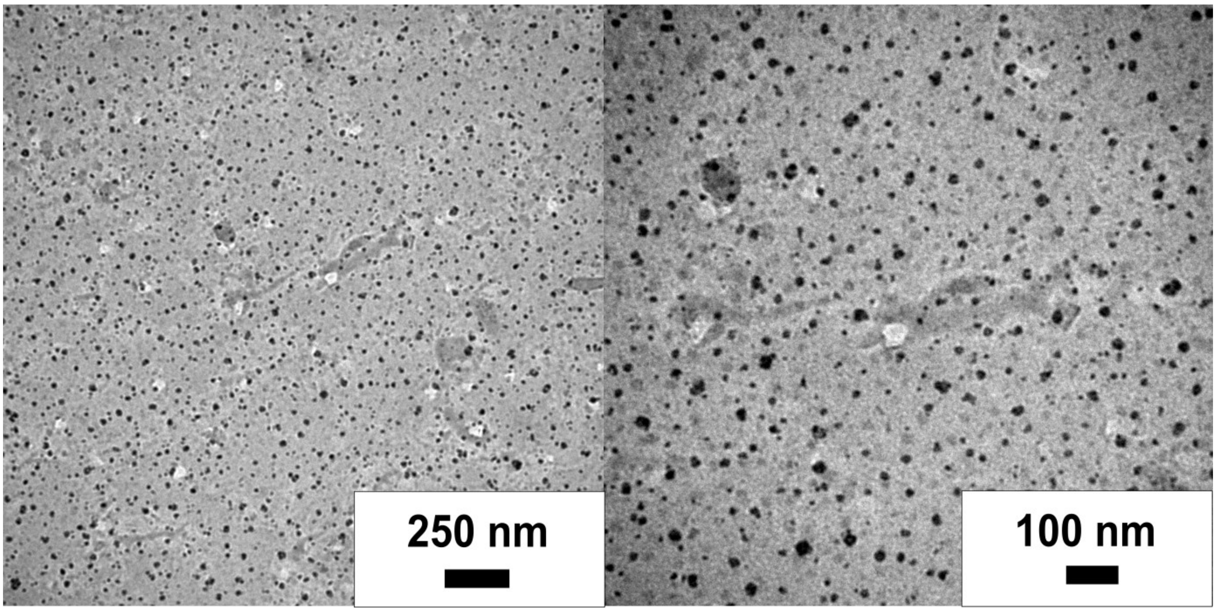

Fig. S14 TEM images of empty BCP micelles of (PMMA$_{13}$-*co*-PDMAEMA$_{22}$)-*b*-PDMAEMA$_{132}$ obtained after drop-casting on carbon-coated copper grids followed by staining with iodine.

Table S2. Comparison of BCPs used in this study with respect to molar ratio (x), weight ratio (w) and volume ratio (θ).

polymer	$x_{PMMA/PDMAEMA}$	$w_{PMMA/PDMAEMA}$	$\theta_{PMMA/PDMAEMA}$[a]
PMMA$_{63}$-*b*-PDMAEMA$_{25}$	72/28	62/38	64/36
PMMA$_{54}$-*b*-PDMAEMA$_{95}$	36/64	27/73	29/71
PMMA$_{19}$-*co*-PDMAEMA$_{22}$	45/55	35/65	37/63
(PMMA$_{19}$-*co*-PDMAEMA$_{22}$)-*b*-PDMAEMA$_{191}$	8/92	5/95	6/94
PMMA$_{13}$-*co*-PDMAEMA$_{22}$	38/62	28/72	30/70
(PMMA$_{13}$-*co*-PDMAEMA$_{22}$)-*b*-PDMAEMA$_{132}$	8/92	5/95	6/94

a) The volume fraction of the block segments was estimated using the densities: 1.18 and 1.32 g cm^{-3} for PMMA and PDMAEMA.

Table S3. Comparison of BCPs used in this study with respect to Zeta potential, Zeta deviation, conductivity and pH.

Micellar solution in water	*Zeta Potential* (mV)	*Zeta Deviation* (mV)	*Conductivity* (mS cm^{-1})	*pH*
[Ru(bipy)$_2$-dppz-7-hydroxymethyl][PF$_6$]$_2$[a]	18.1	4.69	0.564	3.15[c]
PMMA$_{63}$-*b*-PDMAEMA$_{25}$[b]	24.5	6.98	0.129	7.81[d]
PMMA$_{54}$-*b*-PDMAEMA$_{95}$[b]	19.6	3.90	0.131	8.17[e]
(PMMA$_{19}$-*co*-PDMAEMA$_{22}$)-*b*-PDMAEMA$_{191}$[b]	9.6	3.33	0.213	8.50[f]
(PMMA$_{13}$-*co*-PDMAEMA$_{22}$)-*b*-PDMAEMA$_{132}$[b]	13.1	3.49	0.208	8.03[g]

[a] pH determined with a concentration of 1 mg/mL. [b] pH determined with a concentration of 10 mg/mL. [c] pH determined at 22.8 °C. [d] pH determined at 22.4 °C. [e] pH determined at 22.6 °C. [f] pH determined at 22.9 °C. [g] pH determined at 23.5 °C.

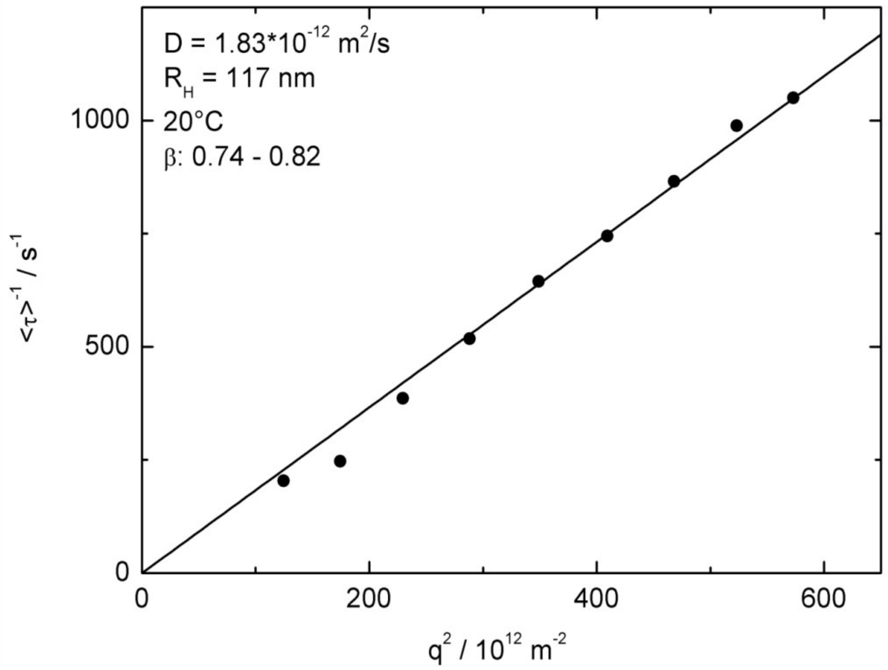

Fig. S15 q^2 dependence of inverse relaxation times to determine diffusion coefficient and resulting hydrodynamic radii for the slow process of the BCP micelles measured at 20 °C.

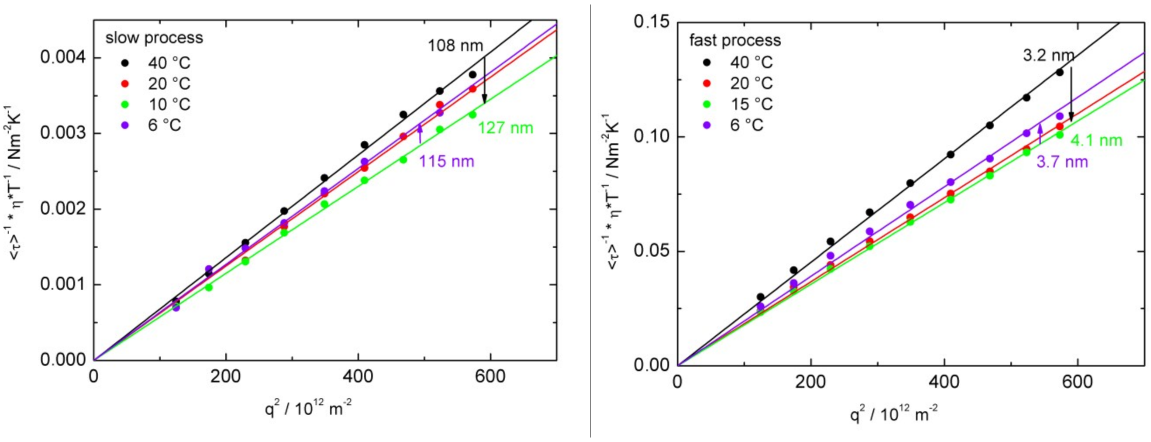

Figure S16. q^2 dependence of scaled inverse relaxation times to determine diffusion coefficient and resultant hydrodynamic radii for the slow process of the aggregates (left) and the fast process of the BCP micelle motions (right), measured in the temperature range of 40 °C – 6 °C.

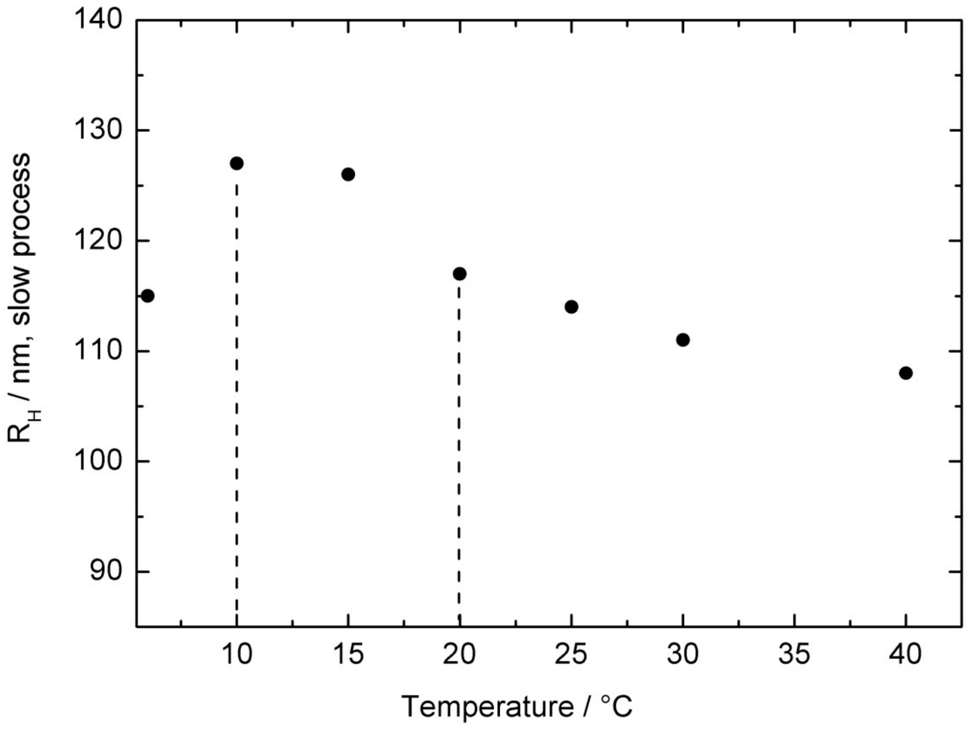

Figure S17. Temperature dependence of hydrodynamic radii of the BCP micelle aggregates in water for polymer ($PMMA_{13}$-*co*-$PDMAEMA_{22}$)-*b*-$PDMAEMA_{132}$.

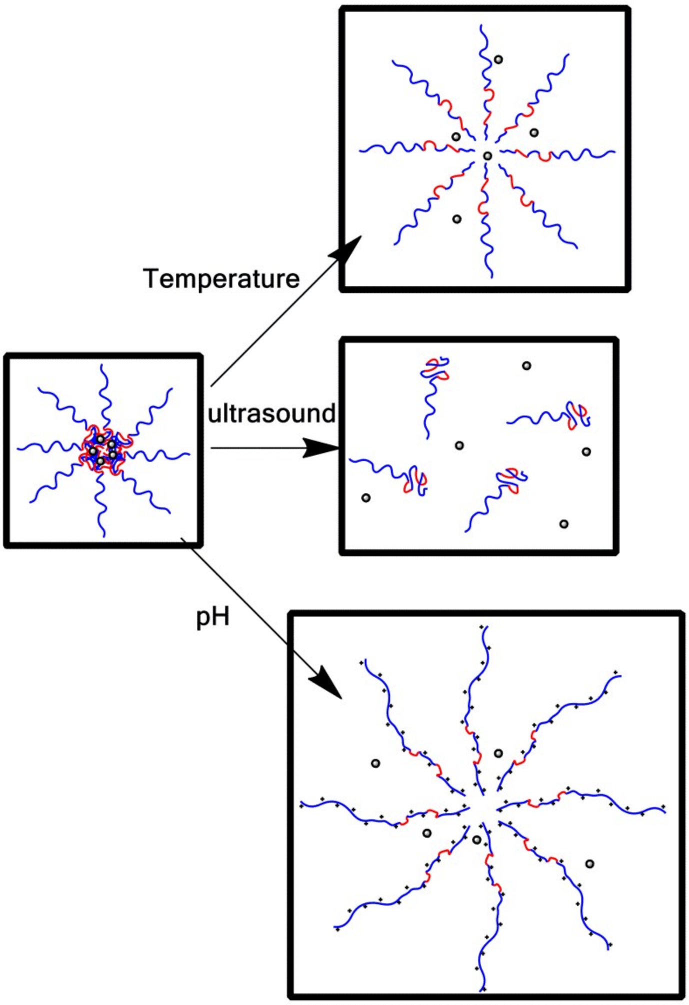

Scheme S1. Simplified scheme for the influence of different external triggers comprising T, ultrasound and pH change to the BCP micelles. While the application of temperature leads to a change of the micelle sizes due to dilution of some part of the statistical block segments (top), ultrasound is expected to dissipate the micelles (followed by reformation of the micelles, see Introduction). Change to lower pH values causes an introduction of charges to the polymer chain, hence diluting the micelles in water which is accompanied with a ruthenium release.

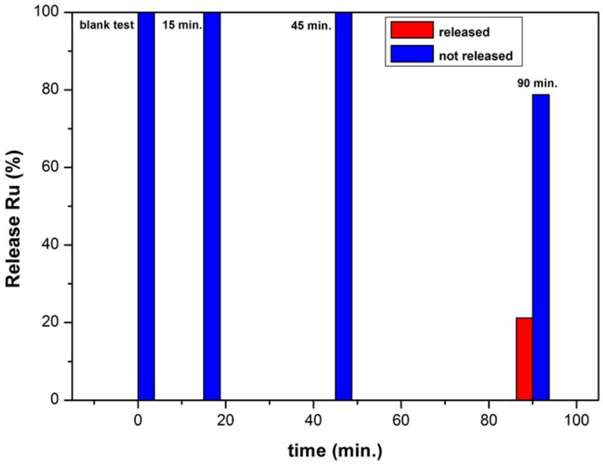

Figure S18 Release profile for BCP micelles loaded with Ru(II) complex **7** based on $PMMA_{54}$-*b*-$PDMAEMA_{95}$ by using ultrasound. The amount of released Ruthenium was determined by AAS.

Table S4. Characterization via AAS of BCPs used in this study with respect to Ru content after different stimuli.

	($PMMA_{19}$-*co*-$PDMAEMA_{22}$)-*b*-$PDMAEMA_{191}$		**($PMMA_{13}$-*co*-$PDMAEMA_{22}$)-*b*-$PDMAEMA_{132}$**	
	Released (µM)	*Not released* (µM)	*Released* (µM)	*Not released* (µM)
ultrasound	84.89	19.72	127.64	0.45
pH	292.45	0.52	178.99	2.92
3 °C	167.09	0.78	110.96	0.63